

# Bragg scattering of surface waves over permeable rippled beds with current

Chao-Lung Ting, Ming-Chung Lin, and Chwen-Ling Kuo

*Department of Naval Architecture and Ocean Engineering, National Taiwan University, Taiwan, Republic of China*

(Received 23 September 1999; accepted 8 March 2000)

In this study we develop a time-dependent wave equation for waves propagating with a current over permeable rippled beds. As well known, Bragg resonance occurs when the incident wavelength is twice the wavelength of the bottom ripple undulation and no current is present. However, the current in the near-shore region changes the resonance condition. A one-dimensional wave field is solved numerically based on the derived equation to study the effect of current on the Bragg resonance condition. Nonlinear wave-wave resonant interaction theory provides an explanation of the effect on Bragg resonance. Numerical results also indicate that the maximum reflection coefficient increases as current velocity increases from a negative to a positive value. Furthermore, the velocity of the current affects the position of the maximum reflection coefficient. © 2000 American Institute of Physics. [S1070-6631(00)02806-3]

## I. INTRODUCTION

In the nearshore region, bottom topography and currents significantly affect wave transformations. Berkhoff<sup>1</sup> assumed the bottom of the sea varies mildly and used the perturbation method to develop the well-known mild-slope equation. Smith and Sprinks<sup>2</sup> used the Green's second identity to derive the same mild-slope equation as that obtained by Berkhoff.<sup>1</sup> However, the equation derived without incorporating current effects may not accurately predict the nearshore wave transformation. Therefore, Booij,<sup>3</sup> Kirby,<sup>4,5</sup> and Liu<sup>6</sup> used different methodologies to obtain the mild-slope equation accounting for the presence of a current. However, the wave transformations over a mild-slope sea bottom with rapidly varying undulations cannot be accurately predicted using the above theory. An intriguing phenomenon called Bragg resonance was found during wave transformations involving this latter bottom topography.

A wave propagating over a wavy mild-slope bottom produces reflected and transmitted waves. When the transmitted wave height is reduced significantly and the reflected wave height grows to its maximum, significant standing waves appear in front of the rippled seabed. This phenomenon is called Bragg resonance. Davies and Heathershaw<sup>7</sup> studied this problem both experimentally and theoretically for a horizontal bottom with sinusoidal undulation. These researchers found their theoretical results well matched with their experimental results. They also highlighted that the Bragg resonance occurs when the wavelength of the incident surface wave is twice that of the bottom undulation. However, their theory breaks down near the Bragg resonance condition. To overcome this drawback, Mei<sup>8</sup> developed wave evolution and reflection theory at and near Bragg resonance condition for shore-parallel sinusoidal bars. Naciri and Mei<sup>9</sup> further studied Bragg scattering by a two-dimensional doubly periodic seabed. Unsatisfied with only knowing the resonance

condition, Kirby<sup>10</sup> derived a more general wave equation to analyze wave transformations over a mildly sloping sea bottom with a rapidly varying undulation. O'Hare and Davies<sup>11</sup> also examined this problem by applying their successive-application-matrix model, and Chamberlain and Porter<sup>12</sup> did the same with their modified mild-slope equation. Meanwhile, Guazzelli *et al.*<sup>13</sup> experimentally investigated higher-order Bragg resonant interactions between linear gravity waves and doubly sinusoidal beds. Recently, Liu and Yue<sup>14</sup> studied generalized Bragg scattering of surface waves over wavy sea bottoms. In their study, a nonlinear wave-wave interaction theory was imposed to analyze different Bragg resonance conditions. They considered different combinations of waves and undulations, including one bottom and two surface wave components, two bottom and two surface wave components, and one bottom and three surface wave components. Apparently, nonlinear wave-wave interaction theory can explain and predict the Bragg scattering very accurately.

In reality, some seabeds may be permeable, and the aforementioned theories that do not account for permeability, cannot describe consequent dissipation. Although Izumiya<sup>15</sup> derived an extended mild-slope equation for a permeable submerged breakwater, the equation is only suitable for a mildly varying bottom slope. Therefore, Mase *et al.*<sup>16</sup> obtained a wave equation for waves propagating over one-dimensional and two-dimensional permeable rippled beds. In their paper, various seabed permeability conditions were considered in some detail. They also demonstrated that permeability causes significant wave energy dissipation. However, their neglect of the presence of currents in the nearshore in their derivation may affect the Bragg resonance condition. Therefore, in this study we derive a more generalized wave equation and to examine numerically how the current affects Bragg resonance.

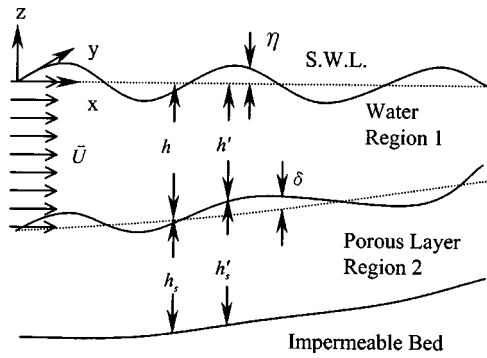


FIG. 1. Definition sketch of the problem.

**II. DERIVATION OF WAVE EQUATION**

Consider surface gravity waves traveling over slowly varying permeable ripple beds with a current (uniform in the  $z$  direction). A definition sketch of the problem is shown in Fig. 1. Cartesian coordinates  $(x, y, z)$  are fixed on the still water level (S.W.L.) with the origin placed at the start of the ripple variation. The free surface elevation is denoted by  $\eta$  and  $\mathbf{U}(x, y)$  represents the current velocity vector. The slowly varying mean water depth,  $h(x, y)$ , is defined as the distance between the S.W.L. and the mean position of the rapidly varying small ripple undulation,  $\delta(x, y)$ . The actual water depth  $h'(x, y)$ , the distance between S.W.L. and  $\delta(x, y)$ , satisfies

$$h'(x, y) = h(x, y) - \delta(x, y). \tag{1}$$

The thickness of the porous layer,  $h'_s(x, y)$ , is the distance between  $\delta(x, y)$  and the impermeable sea bottom. Thus, the slowly varying mean thickness of the porous layer,  $h_s(x, y)$ , can be described by

$$h_s(x, y) = h'_s(x, y) - \delta(x, y). \tag{2}$$

The following assumptions are made:

$$O\left(\frac{\nabla h}{kh}\right) \approx O(k\delta) \ll 1, \tag{3}$$

$$O\left(\frac{\nabla(h+h_s)}{kh}\right) \approx O(k\delta) \ll 1, \tag{4}$$

and

$$O\left(\frac{\nabla \delta}{k\delta}\right) \approx O(1), \tag{5}$$

where  $\nabla$  denotes the horizontal gradient operator ( $\partial/\partial x, \partial/\partial y$ ), and  $k$  represents the wave number. The domain of interest consists of two regions. Region 1 is the fluid domain above region 2, which latter region represents the porous layer lying above the impermeable sea bottom, as shown in Fig. 1.

In region 1, the fluid is assumed to be inviscid and incompressible, and the wave motion is irrotational. In this region, the mean current velocity vector,  $\mathbf{U}(x, y)$ , coexists with small-amplitude wave motion, which is represented by the velocity potential,  $\Phi_w(x, y, z, t)$ . The magnitude of  $\mathbf{U}(x, y)$ , of  $O(1)$ , is greater than the magnitude of wave

velocity, of  $O(\epsilon)$ , where  $\epsilon = ka$  (the wave steepness) is assumed to be small [i.e.,  $O(\epsilon) \ll 1$ ]. Accordingly, the total velocity can be represented by

$$\mathbf{V}(x, y, z, t) = \mathbf{U}(x, y) + \epsilon \nabla_3 \Phi_w(x, y, z, t), \tag{6}$$

and the free-surface displacement is written as

$$\eta = \epsilon \eta_w(x, y, t), \tag{7}$$

where  $\nabla_3 = (\partial/\partial x, \partial/\partial y, \partial/\partial z)$ . Here,  $\mathbf{U}(x, y)$  is given as a mean velocity vector without variations in the  $z$  direction, and satisfies the zeroth-order boundary value problem [i.e.  $O(\epsilon^0)$ ], such that discussion of the  $O(\epsilon^0)$  problem is excluded.

Upon substitution of Eq. (6) into the continuity equation, the linearized governing equation and boundary conditions of  $O(\epsilon^1)$  in region 1 are obtained as follows:

$$\nabla^2 \Phi_w + \frac{\partial^2 \Phi_w}{\partial z^2} = 0, \quad -h \leq z \leq 0; \tag{8}$$

$$\frac{D^2 \Phi_w}{Dt^2} + g \frac{\partial \Phi_w}{\partial z} = 0, \quad z = 0; \tag{9}$$

$$\frac{\partial \Phi_w}{\partial z} + \nabla \Phi_w \cdot \nabla h - \nabla \cdot (\delta \nabla \Phi_w) = W^{(1)}, \quad z = -h; \tag{10}$$

$$P_1^{(1)} = -\rho \left( \frac{\partial \Phi_w}{\partial t} + \mathbf{U} \cdot \nabla \Phi_w \right), \quad z = -h. \tag{11}$$

Equation (8) is the governing equation. Equation (9) represents the combined free surface boundary condition, where the total derivative is defined as

$$\frac{D^2}{Dt^2} = \left( \frac{\partial}{\partial t} + \bar{\mathbf{U}} \cdot \nabla \right) \left( \frac{\partial}{\partial t} + \mathbf{U} \cdot \nabla \right). \tag{12}$$

Equation (10) is the kinematic permeable bottom boundary condition, where  $W^{(1)}$  is the discharge velocity at the interface  $z = -h$ . At  $z = -h$  in region 1, the pressure denoted by  $P_1^{(1)}$  is given by Eq. (11).

In region 2, the fluid is also assumed to be irrotational. The flow motion in this porous layer is mainly due to the wave motion in region 1, since the mean current effect is negligible. Adopting the momentum equation used by Sollitt and Cross<sup>17</sup> and Mase *et al.*<sup>16</sup> and following the same procedure as that used for region 1, we obtain the governing equation and boundary conditions of  $O(\epsilon^1)$  in region 2 as follows:

$$\nabla^2 \Psi + \frac{\partial^2 \Psi}{\partial z^2} = 0, \quad -(h+h_s) \leq z \leq -h; \tag{13}$$

$$\frac{\partial \Psi}{\partial z} + \nabla \Psi \cdot \nabla h - \nabla \cdot (\delta \nabla \Psi) = W^{(2)}, \quad z = -h; \tag{14}$$

$$P_1^{(2)} = -\rho \left( \frac{\tau}{n} \frac{\partial \Psi}{\partial t} + f \frac{\omega}{n} \Psi \right), \quad z = -h; \tag{15}$$

$$\frac{\partial \Psi}{\partial z} = -\nabla \Psi \cdot \nabla (h+h_s), \quad z = -(h+h_s), \tag{16}$$

where  $\Psi$  is defined as the discharge velocity potential,  $n$  is the porosity,  $\tau$  is the inertia coefficient,  $f$  is the linearized friction factor, and  $\omega$  is the absolute angular frequency. At the interface  $z = -h$ , the kinematic and dynamic permeable boundary conditions are given by Eq. (14) and Eq. (15), respectively.  $W^{(2)}$  is the discharge velocity at the interface between region 2 and region 1.  $P_1^{(2)}$  is the first-order pressure in region (2). Equation (16) is the bottom boundary condition at the impermeable sea bottom.

At the interface  $z = -h$ , the pressure and the vertical discharge velocity should be continuous; therefore, the following conditions must be met:

$$P_1^{(1)} = P_1^{(2)}, \quad z = -h, \tag{17}$$

and

$$W_1^{(1)} = W_1^{(2)}, \quad z = -h. \tag{18}$$

Using Eqs. (10), (11), (15), and (16), Eqs. (17) and (18) can be rewritten as

$$\frac{\partial \Phi_w}{\partial t} + \mathbf{U} \cdot \nabla \Phi_w = \frac{\tau}{n} \frac{\partial \Psi}{\partial t} + f \frac{\omega}{n} \Psi, \quad z = -h, \tag{19}$$

$$\begin{aligned} \frac{\partial \Phi_w}{\partial z} + \nabla \Phi_w \cdot \nabla h - \nabla \cdot (\delta \nabla \Phi_w) \\ = \frac{\partial \Psi}{\partial z} + \nabla \Psi \cdot \nabla h - \nabla \cdot (\delta \nabla \Psi), \quad z = -h. \end{aligned} \tag{20}$$

By analogy to the solutions from Mase *et al.*,<sup>16</sup> we assume the solutions for velocity potentials,  $\Phi_w$  and  $\Psi$ , as follows:

$$\begin{aligned} \Phi_w(x, y, z, t) = f^{(1)}(x, y, z) \tilde{\phi}(x, y, t) \\ + (\text{nonpropagating modes}), \end{aligned} \tag{21}$$

$$\begin{aligned} \Psi(x, y, z, t) = f^{(2)}(x, y, z) \tilde{\varphi}(x, y, t) \\ + (\text{nonpropagating modes}). \end{aligned} \tag{22}$$

Since nonpropagating modes (evanescent modes) are not relevant to this study, a discussion is not given herein.

To obtain the vertical distribution functions of  $f^{(1)}$  and  $f^{(2)}$ , we follow the derivation procedures used in Gu and Wang<sup>18</sup> and assume a horizontal bottom (i.e.,  $\nabla h = \nabla h_s = 0$ ). Then, the expressions of  $f^{(1)}$  and  $f^{(2)}$  can be obtained as follows:

$$\begin{aligned} f^{(1)} = \frac{1}{Q} \left[ \frac{\omega}{\sigma} \cosh kh_s \cosh k(h+z) \right. \\ \left. + \gamma \sinh kh_s \sinh k(h+z) \right], \end{aligned} \tag{23}$$

$$f^{(2)} = \frac{1}{Q} \gamma \cosh k(h+h_s+z), \tag{24}$$

where

$$\sigma = \omega - \mathbf{k} \cdot \mathbf{U} \quad (\text{the intrinsic frequency}), \tag{25}$$

$$Q = \cosh kh_s \cosh kh \left( \frac{\omega}{\sigma} + \gamma \tanh kh_s \tanh kh \right), \tag{26}$$

$$\gamma = \frac{n}{\tau + if}, \tag{27}$$

and  $i$  is the imaginary unity. Also, the dispersion relation is obtained:

$$\sigma^2 = gk \frac{\frac{\omega}{\sigma} \tanh kh + \gamma \tanh kh_s}{\frac{\omega}{\sigma} + \gamma \tanh kh \tanh kh_s}. \tag{28}$$

Substituting Eqs. (21) and (22) into Eq. (19) and considering only propagating modes, yields

$$\tilde{\phi} = \tilde{\varphi}. \tag{29}$$

Following Smith and Sprinks,<sup>2</sup> Kirby,<sup>10</sup> and Mase *et al.*<sup>16</sup> and using the Green's second identity for  $\Phi_w$  and  $f^{(1)}$ , Eq. (30) can be obtained; thus

$$\begin{aligned} \int_{-h}^0 f^{(1)} \frac{\partial^2 \Phi_w}{\partial z^2} dz - \int_{-h}^0 \frac{\partial^2 f^{(1)}}{\partial z^2} \Phi_w dz \\ = \left( f^{(1)} \frac{\partial \Phi_w}{\partial z} - \frac{\partial f^{(1)}}{\partial z} \Phi_w \right) \Big|_{-h}. \end{aligned} \tag{30}$$

Integrating the above equation, we can obtain Eq. (31) by applying the boundary conditions and neglecting the high-order terms of the bottom slope:

$$\begin{aligned} \nabla \cdot \int_{-h}^0 f^{(1)2} \nabla \tilde{\phi} dz + k^2 \int_{-h}^0 f^{(1)2} \tilde{\phi} dz \\ = \frac{1}{g} \left( \frac{D^2 \tilde{\phi}}{Dt^2} + (\nabla \cdot \mathbf{U}) \frac{D \tilde{\phi}}{Dt} + \sigma^2 \tilde{\phi} \right) + f^{(1)2} \nabla \cdot (\delta \nabla \tilde{\phi}) \Big|_{-h} \\ + f^{(1)} W^{(1)} \Big|_{-h} - \tilde{\phi} f^{(1)} \frac{\partial f^{(1)}}{\partial z} \Big|_{-h}. \end{aligned} \tag{31}$$

Similarly, applying the Green's second identity for  $\Psi$  and  $f^{(2)}$  yields

$$\begin{aligned} \int_{-(h+h_s)}^{-h} f^{(2)} \frac{\partial^2 \Psi}{\partial z^2} dz - \int_{-(h+h_s)}^{-h} \frac{\partial^2 f^{(2)}}{\partial z^2} \Psi dz \\ = \left( f^{(2)} \frac{\partial \Psi}{\partial z} - \frac{\partial f^{(2)}}{\partial z} \Psi \right) \Big|_{-(h+h_s)}, \end{aligned} \tag{32}$$

and the integration gives us

$$\begin{aligned} \nabla \cdot \int_{-(h+h_s)}^{-h} f^{(2)2} \nabla \tilde{\varphi} dz + k^2 \int_{(h+h_s)}^{-h} f^{(2)2} \tilde{\varphi} dz \\ = -f^{(2)2} \nabla \cdot (\delta \nabla \tilde{\varphi}) \Big|_{-h} - f^{(2)} W^{(2)} \Big|_{-h} + \tilde{\varphi} f^{(2)} \frac{\partial f^{(2)}}{\partial z} \Big|_{-h}. \end{aligned} \tag{33}$$

Using the relation  $W^{(1)} = W^{(2)}$  with  $\tilde{\phi} = \tilde{\varphi}$  to combine Eqs. (31) and (33), we obtain

$$\frac{D^2 \tilde{\phi}}{Dt^2} + (\sigma^2 - \alpha k^2) \tilde{\phi} - \nabla \cdot (\alpha \nabla \tilde{\phi}) - \frac{g}{Q^2} \cosh kh_s \frac{\omega}{\sigma} \left( \frac{\omega}{\sigma} - \gamma \right) \nabla \cdot (\delta \nabla \tilde{\phi}) = 0, \quad (34)$$

where

$$\alpha = g \left( p + \frac{\omega}{\sigma} \frac{q}{\gamma} \right), \quad (35)$$

$$p = \int_{-h}^0 f^{(1)2} dz = [(\omega/\sigma)^2 \cosh^2 kh_s (\sinh 2kh + 2kh) + \gamma^2 \sinh^2 kh_s (\sinh 2kh - 2kh) + (\omega/\sigma) \gamma \sinh 2kh_s (\cosh 2kh - 1)]/4/k/Q^2, \quad (36)$$

$$q = \int_{-(h+h_s)}^{-h} f^{(2)2} dz = \gamma^2 (\sinh 2kh_s + 2kh_s)/4/k/Q^2. \quad (37)$$

If  $\mathbf{U}=0$  (i.e., there is no current in the wave field), Eq. (34) reduces to

$$\frac{\partial^2 \tilde{\phi}}{\partial t^2} + (\omega^2 - \alpha k^2) \tilde{\phi} - \nabla \cdot (\alpha \nabla \tilde{\phi}) - \frac{g}{Q^2} \cosh kh_s (1 - \gamma) \nabla \cdot (\delta \nabla \tilde{\phi}) = 0, \quad (38)$$

with the dispersion relation

$$\omega^2 = gk \frac{\tanh kh + \gamma \tanh kh_s}{1 + \gamma \tanh kh \tanh kh_s}, \quad (39)$$

which is the same as the equations obtained by Mase *et al.*<sup>16</sup> If there are no porous layers and no undulation on the bottom (i.e.,  $h_s=0$  and  $\delta=0$ ), Eq. (35) reduces to

$$\alpha = \frac{\sigma^2}{2k^2} \left( 1 + \frac{2kh}{\sinh 2kh} \right) = CC_g, \quad (40)$$

and Eq. (34) becomes

$$\frac{D^2 \tilde{\phi}}{Dt^2} + (\sigma^2 - k^2 CC_g) \tilde{\phi} - \nabla \cdot (CC_g \nabla \tilde{\phi}) = 0, \quad (41)$$

with the dispersion relation

$$\sigma^2 = (\omega - \mathbf{k} \cdot \mathbf{U})^2 = gk \tanh kh, \quad (42)$$

which is the well-known mild-slope equation with current. To simplify the problem, assumption have been made. A monochromatic wave interacting with a current was considered one-dimensionally. Also,  $O(\alpha/|\mathbf{U}|^2) \gg 1$  ( $\alpha$  has the same physical meaning as  $CC_g$ ) is assumed to reduce the original equation to a simple and solvable form. Therefore, Eq. (35) can be written as

$$\phi_{xx} + \nu^{-1} (\alpha_x + M \delta_x + 2i\omega U) \phi_x + \nu^{-1} (\omega^2 - \sigma^2 + \alpha k^2) \phi = 0, \quad (43)$$

where

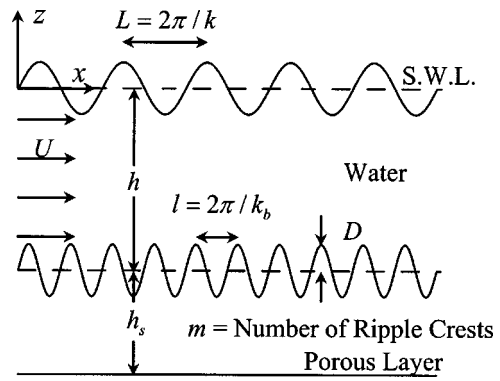


FIG. 2. Definition sketch of the sinusoidal undulations.

$$M = \frac{g}{Q^2} \cosh kh_s \frac{\omega}{\sigma} \left( \frac{\omega}{\sigma} - \gamma \right) \quad (44)$$

and

$$\nu = \alpha + M \delta. \quad (45)$$

Numerical results and discussions follows, according to the above equation.

### III. NUMERICAL RESULTS AND DISCUSSIONS

Since Eq. (43) is an elliptic-type equation, its solution requires closed boundary conditions in an analytical domain. However, in the present problem, shoreward boundary conditions cannot be known *a priori*. Therefore, the approximation method proposed by Radder<sup>19</sup> and Kirby<sup>10</sup> is adopted to transform the elliptic-type equation into coupled parabolic equations for forward- and backward-scattered waves. The transformation allows the problem to be solved numerically. Numerical results for the no current situation were reproduced to verify the present model. Our results agree significantly with results from Kirby<sup>10</sup> and Mase *et al.*<sup>16</sup>

The ripple bed models used in all tests are the same as those shown in Fig. 2. The mean water depth  $h$  and the mean thickness of porous layer  $h_s$  are kept constant. The small ripple undulation  $\delta$  is given by

$$\delta = D \sin k_b x, \quad 0 \leq x \leq ml, \quad (46)$$

where  $k_b$ ,  $l$ ,  $D$  and  $m$  are the wave number, the wavelength, the amplitude of ripples, and the number of ripples, respectively. Numerical calculations were carried out with different current velocities,  $U$ , and permeability conditions. However, the conditions,  $l=1$  m,  $D=0.05$  m,  $m=4$ ,  $D/h=0.32$ ,  $n=0.4$ , and  $\tau=1.0$  remain fixed in all tests. The calculated reflection coefficient  $R$  and transmission coefficient  $T$  are defined as

$$R = \frac{|B_{x=0}|}{a_0}, \quad T = \frac{|A_{x=ml}|}{a_0}, \quad (47)$$

where  $a_0$  is the incident wave amplitude,  $A_{x=ml}$  is the transmitted wave amplitude measured at  $x=ml$ , and  $B_{x=0}$  is the reflected wave amplitude measured at  $x=0$ .

The incident wave condition is described by the relative wave number  $2k/k_b$  ( $\equiv$ twice the ratio of transmitted wave

number and ripple wave number), ranging from 0.5 to 2.5 in all numerical calculations. However, in the permeable bottom case, the transmitted wave number measured above the ripple bed is complex ( $=k_{\text{real}} + ik_{\text{imag}}$ ). Therefore, the  $k$  used in the relative wave number is simply the real part of the transmitted wave number,  $k_{\text{real}}$ .

Bragg resonance of different permeable bed conditions with zero current velocity were fully discussed in Ref. 16. Therefore, the zero-current-velocity case is not discussed here in detail. Rather, we focus on the change of the Bragg resonance conditions due to the presence of current.

Various combinations of numerical conditions were tested by the proposed model. Apparently, the linearized friction factor  $f$  and the mean thickness of the porous layer  $h_s$  negligibly affect the resonance condition. They only affect the magnitude of the reflection coefficient. However, current velocity affects significantly the location of the resonant relative wave number  $(2k/k_b)_r$  ( $\equiv$  the value of  $2k/k_b$  at which the reflection coefficient is maximal). To see how current velocity affects resonance, various current velocities were tested numerically.

The effect of typical values of  $U$  on Bragg resonance is shown in Fig. 3, where  $h_s=0.2$  m remains unchanged in all test conditions. Three subgraphs, (a)–(c), in Fig. 3 represent the results for  $U=-0.15$ , 0, and 0.15 m/s, respectively. The ordinates of each subgraph represents the values of  $R$  and  $T$  and the abscissa represents the value of  $2k/k_b$ . Each subgraph is composed of eight lines. Two of them with the same type of line type represent the effects of a specific permeable condition. The upper line of the two lines represents the  $T$  curve and the lower is the  $R$  curve. The line types from top to bottom represent the results for impermeable,  $f=10$ ,  $f=5$ , and  $f=1$  conditions, respectively.

Figure 3 obviously reveals that the maximum value of  $R$  and  $T$  occur in impermeable case for a given  $2k/k_b$  and that they decrease as  $f$  decreases. Also, the same conclusion as that given by Mase *et al.*<sup>16</sup> is obtained: the minimum values of  $R$  and  $T$  occur under  $f=1$  condition, at which energy dissipation is maximum. In Fig. 3(b), when  $U=0$ , the resonant reflection coefficient  $R_r$  ( $\equiv$  maximum  $R$ ) occurs at  $(2k/k_b)_r \approx 1$ . However, when  $U \neq 0$ ,  $R_r$  occurs at  $(2k/k_b)_r \neq 1$ , as can be seen in Figs. 3(a) and 3(c). Figure 3(a) indicates that  $R_r$  occurs at  $(2k/k_b)_r > 1$  when  $U < 0$  (i.e., current moves in the opposite direction to that of the transmitted wave). Figure 3(c) shows that  $R_r$  occurs at  $(2k/k_b)_r < 1$  when  $U > 0$  (i.e., current moves in the same direction as the transmitted wave). Also, we can see that  $R_r$  increases as  $U$  increases from a negative to a positive value. Therefore, the current velocity does affect the Bragg resonance condition. An explanation of the shift of  $(2k/k_b)_r$  due to the current effect is given in the following paragraphs.

Liu and Yue<sup>14</sup> explained the mechanism of Bragg resonance very well using nonlinear (surface) wave-wave resonant interactions in the absence of bottom undulations. Here, our condition is similar to their class I Bragg condition. Therefore, three-wave resonance is imposed here to elucidate our Bragg resonance with a current present.

Consider the case of an impermeable sea bottom, where  $k_i$  is the transmitted wave number,  $k_r$  is the reflected wave

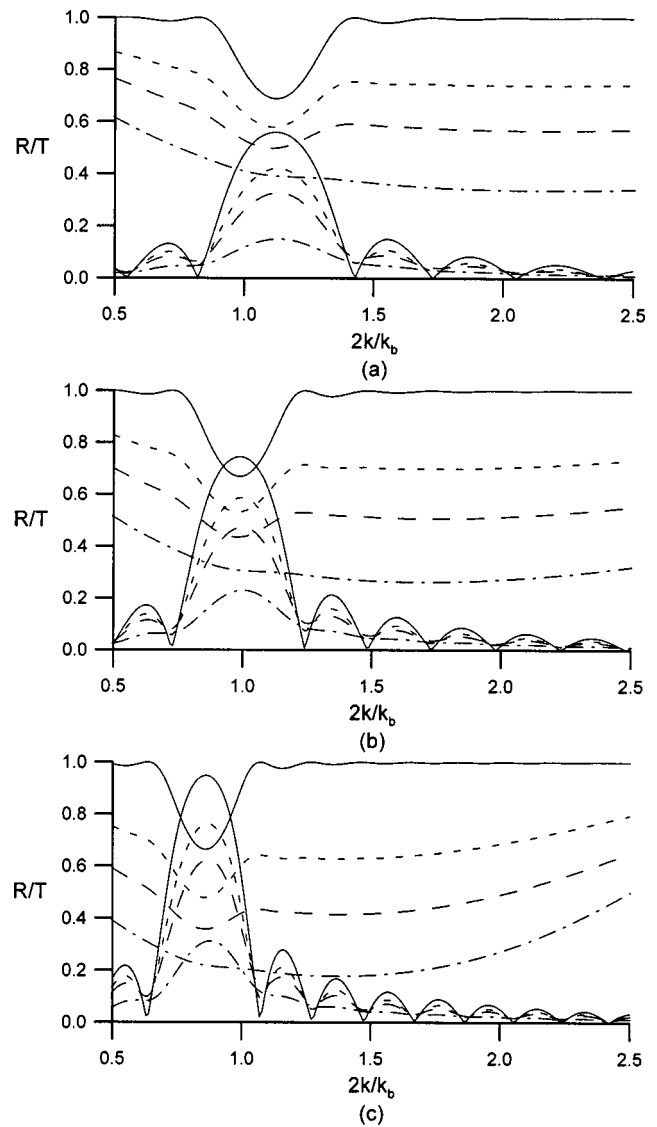


FIG. 3. Effect of currents on the reflection and transmission coefficients over the sinusoidal ripple bottom for the case of  $m=4$ ,  $h_s=0.2$  m, and  $D/h=0.32$ . (a)  $U=-0.15$  m/s, (b)  $U=0$  m/s, (c)  $U=0.15$  m/s. [—: impermeable, ---: permeable ( $f=10$ ), - - - -: permeable ( $f=5$ ), ····: permeable ( $f=1$ ).]

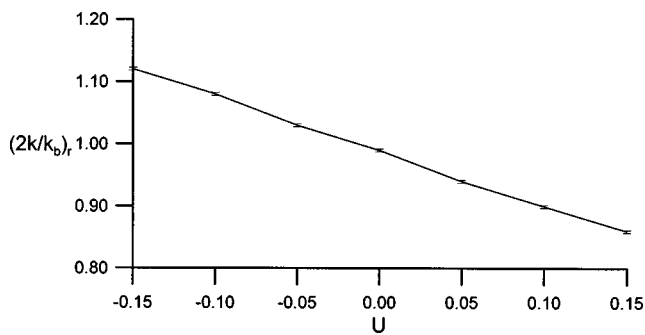
number, and  $k_b$  is the wave number of bottom undulation. The associated angular frequencies are  $\omega_i$ ,  $\omega_r$ , and 0. The following equations must be satisfied to obtain the Bragg resonance:

$$\mathbf{k}_i - \mathbf{k}_r - k_b = 0, \quad (48)$$

$$\omega_i - \omega_r = 0. \quad (49)$$

In the case of  $U=0$ , Eq. (49) implies  $|\mathbf{k}_i| = |\mathbf{k}_r|$ . Therefore, resonance occurs when  $k_b = |\mathbf{k}_i| + |\mathbf{k}_r| = 2|\mathbf{k}_i| = 2k_i$ , i.e.,  $(2k/k_b)_r = 1$ . When  $U > 0$ , Eq. (49) implies  $|k_i| < |k_r|$ . Equation (48) dictates  $k_b = |\mathbf{k}_i| + |\mathbf{k}_r| > 2|\mathbf{k}_i| = 2k_i$ , which implies resonance occurs as  $(2k/k_b)_r < 1$ . Similarly, it is expected that Bragg resonance occurs at  $(2k/k_b)_r > 1$  for  $U < 0$ . Our numerical results clearly accord with this explanation.

Seven different current velocities from  $-0.15$  to 0.15 m/s are used in the numerical tests to determine how current

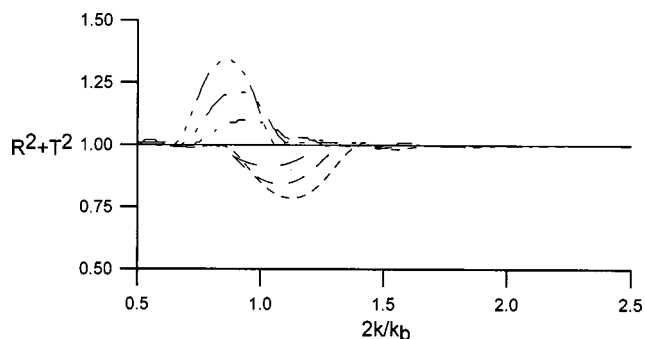
FIG. 4. The effects of current  $U$  on  $(2k/k_b)_r$ .

velocity affects the resonant relative wave number  $(2k/k_b)_r$ . Figure 4 summarizes those results, indicating that  $(2k/k_b)_r$  decreases as  $U$  increases. Also, the numerical calculations show that the linearized friction factor  $f$ , the mean thickness of porous layer  $h_s$ , and the inertial coefficient  $\tau$  have negligible effects on  $(2k/k_b)_r$ .

To investigate the current effect on normalized total wave energy,  $R^2 + T^2$ , this study calculates seven different current velocities for the case of an impermeable bottom, as shown in Fig. 3. Figure 5 displays the resulting  $R^2 + T^2$ . In this figure, seven lines from top to bottom represent the results for  $U = 0.15, 0.10, 0.05, 0, -0.05, -0.10,$  and  $-0.15$  m/s, respectively. As expected, when total wave energy is conserved for the zero-current case, the value of  $R^2 + T^2$  equals one, as the solid line in Fig. 5 displays. The figure also indicates that current significantly affects total wave energy when resonance occurs. Near the resonance region (that is, when significant reflection occurs),  $R^2 + T^2 > 1$  when  $U > 0$  and  $R^2 + T^2 < 1$  when  $U < 0$ . Obviously the value of  $R^2 + T^2$  increases as  $U$  increases from negative to positive. When away from the resonance region (that is, in the region of small reflection),  $R^2 + T^2$  remains one, meaning the current effect on total wave energy is negligible.

#### IV. CONCLUSIONS

Mase *et al.*<sup>16</sup> discussed in detail the one- and two-dimensional wave transformations over a permeable ripple bottom with rapidly varying undulations. However, currents are always present in the near-shore region, e.g., tidal cur-

FIG. 5. The effect of currents on the normalized total wave energy,  $R^2 + T^2$ . Seven line types from top to bottom represent the results for  $U = 0.15, 0.10, 0.05, 0, -0.05, -0.10,$  and  $-0.15$  m/s, respectively.

rents, longshore currents. The prediction of near-shore wave transformation without considering the presence of those currents, may thus be inaccurate. Therefore, to mimic the real near-shore wave transformation, more general wave equations were derived for the wave propagation over seabeds with rapidly varying undulation and currents.

Various conditions were examined by the present numerical model. According to our numerical results, the current does affect the Bragg resonance condition. As  $U > 0$ , the maximum reflection coefficient  $R_r$  occurs at  $(2k/k_b)_r < 1$ . When  $U = 0$ ,  $R_r$  occurs at  $(2k/k_b)_r \approx 1$  and  $R_r$  occurs at  $(2k/k_b)_r > 1$  when  $U < 0$ . The shift of  $(2k/k_b)_r$  is also well explained by the nonlinear three-wave interaction theory mentioned by Liu and Yue.<sup>14</sup> From our results, it is known that  $R_r$  increases as  $U$  increases from a negative to a positive value. However, the current obviously does not affect  $T_r$ . Near the resonance region, the current also significantly influences the normalized total wave energy,  $R^2 + T^2$ .  $R^2 + T^2 > 1$  when  $U > 0$  and  $R^2 + T^2 < 1$  when  $U < 0$ .

The present study can be applied to the design of an artificial sandbar in a near-shore region to protect the shore from wave attack. Figure 3 shows that suitable permeability of the ripple bottom may significantly reduce  $R_r$  and  $T_r$ . Therefore, we recommend that using a permeable material (with suitable friction factor) to manufacture artificial ripple bottoms should be an effective way to reduce the height of transmitted waves.

#### ACKNOWLEDGMENTS

The authors would like to thank Professor Ching-Piao Tsai (Department of Civil Engineering, National Chung-Hsing University, Taiwan) and Professor Tai-wen Hsu (Department of Hydraulics and Ocean Engineering, National Cheng-Kung University, Taiwan) for their helpful discussions.

- <sup>1</sup>J. C. W. Berkhoff, "Computation of combined refraction-diffraction," *Proceedings of the 13th International Conference on Coastal Engineering*, ASCE, 1972, p. 471.
- <sup>2</sup>R. Smith and T. Sprinks, "Scattering of surface waves by conical island," *J. Fluid Mech.* **72**, 373 (1975).
- <sup>3</sup>N. Booij, "Gravity waves on water with non-uniform depth and current," Report No. 81-1, Delft Univ. of Tech., Holland, 1981.
- <sup>4</sup>J. T. Kirby, "Propagation of weakly-nonlinear surface water waves in regions with varying depth and currents." Ph.D. thesis, Department of Civil Engineering, University of Delaware, 1983.
- <sup>5</sup>J. T. Kirby, "A note on linear surface wave-current interaction over slowly varying topography," *J. Geophys. Res.* **89**, 745 (1984).
- <sup>6</sup>P. L.-F. Liu, "Wave-current interactions on a slowly varying topography," *J. Geophys. Res.* **88**, 4421 (1983).
- <sup>7</sup>A. G. Davies and A. D. Heathershaw, "Surface-wave propagation over sinusoidally varying topography," *J. Fluid Mech.* **144**, 828 (1984).
- <sup>8</sup>C. C. Mei, "Resonant reflection of surface waves by periodic sandbars," *J. Fluid Mech.* **152**, 315 (1985).
- <sup>9</sup>M. Naciri and C. C. Mei, "Bragg scattering of water waves by a doubly periodic seabed," *J. Fluid Mech.* **192**, 159 (1988).
- <sup>10</sup>J. T. Kirby, "A general wave equation for rippled beds," *J. Fluid Mech.* **162**, 171 (1986).
- <sup>11</sup>T. J. O'Hare and A. G. Davies, "A comparison of two models for surface-wave propagation over rapidly varying topography," *Appl. Ocean Res.* **15**, 1 (1993).
- <sup>12</sup>P. G. Chamberlain and D. Porter, "The modified mild-slope equation," *J. Fluid Mech.* **291**, 393 (1995).

- <sup>13</sup>E. Guazzelli, V. Rey, and M. Belzons, "Higher-order Bragg reflection of gravity surface waves by periodic beds," *J. Fluid Mech.* **245**, 301 (1992).
- <sup>14</sup>Y. Liu and D. K. P. Yue, "On generalized Bragg scattering of surface waves by bottom ripples," *J. Fluid Mech.* **356**, 297 (1998).
- <sup>15</sup>T. Izumiya, "Extension of mild slope equation for waves propagating over a permeable submerged breakwater," *Proceedings of the 22nd International Conference on Coastal Engineering*, ASCE, 1990, p. 306.
- <sup>16</sup>H. Mase, K. Takeba, and S. I. Oki, "Wave equation over permeable rippled bed and analysis of Bragg scattering of surface gravity waves," *J. Hydraul. Res.* **27**, 587 (1995).
- <sup>17</sup>C. K. Sollitt and R. H. Cross, "Wave transmission through permeable breakwaters," in Ref. 1, p. 1827.
- <sup>18</sup>Z. Gu and H. Wang, "Gravity wave over porous bottoms," *Coastal Eng.* **15**, 497 (1991).
- <sup>19</sup>A. C. Radder, "On the parabolic equation method for water wave propagation," *J. Fluid Mech.* **95**, 159 (1979).